Cancer Letters 448 (2019) 70–83

Contents lists available at ScienceDirect

Cancer Letters

journal homepage: www.elsevier.com/locate/canlet

Original Articles

# Proteasome inhibitor b-AP15 induces enhanced proteotoxicity by inhibiting cytoprotective aggresome formation

Ellin-Kristina Hillert[a], Slavica Brnjic[a], Xiaonan Zhang[a], Magdalena Mazurkiewicz[a], Amir Ata Saei[b], Arjan Mofers[c], Karthik Selvaraju[c], Roman Zubarev[b], Stig Linder[a,c], Padraig D'Arcy[a,c,*]

[a] Department of Oncology-Pathology, Karolinska Institute, Stockholm, Sweden
[b] Department of Medical Biochemistry and Biophysics, Karolinska Institute, Stockholm, Sweden
[c] Department of Medical and Health Sciences, Linköping University, Linköping, Sweden

ARTICLE INFO

*Keywords:*
Ubiquitin-proteasome system
Deubiquitinase
UPS inhibitor

ABSTRACT

Proteasome inhibitors have been shown to induce cell death in cancer cells by triggering an acute proteotoxic stress response characterized by accumulation of poly-ubiquitinated proteins, ER stress and the production of reactive oxygen species. The aggresome pathway has been described as an escape mechanism from proteotoxicity by sequestering toxic cellular aggregates. Here we show that b-AP15, a small-molecule inhibitor of proteasomal deubiquitinase activity, induces poly-ubiquitin accumulation in absence of aggresome formation. b-AP15 was found to affect organelle transport in treated cells, raising the possibility that microtubule-transport of toxic protein aggregates is inhibited, leading to enhanced cytotoxicity. In contrast to the antiproliferative effects of the clinically used proteasome inhibitor bortezomib, the effects of b-AP15 are not further enhanced by the histone deacetylase inhibitor suberoylanilide hydroxamic acid (SAHA). Our results suggest an inhibitory effect of b-AP15 on the transport of misfolded proteins, resulting in a lack of aggresome formation, and a strong proteotoxic stress response.

## 1. Introduction

The Ubiquitin-Proteasome system. The accumulation and aggregation of mis-folded or damaged proteins is a common occurrence in the life of a cell, and is of particular importance in many neurodegenerative disorders and cancers, where it can lead to deleterious consequences [1]. This accumulation can be induced by changes in protein structure due to mutations and alterations to RNA, as well as thermal and oxidative stress [2,3]. Protein quality control in the cell is primarily mediated by the ubiquitin-proteasome system (UPS) [4]. Misfolded, damaged or temporally regulated proteins are marked for removal by the small protein ubiquitin, which functions as a destruction-tag, causing the substrate to be trafficked to the 26S proteasome, where degradation occurs. The process is highly dynamic, tightly regulated, and involves multiple ubiquitination and de-ubiquitination steps. Once at the 26S proteasome, poly-ubiquitinated proteins are processed by three deubiquitinase (DUB) enzymes associated with the 19S regulatory particle (19S RP) - USP14, UCHL5 and POH1 [5–7]. The proteasomal DUBs remove the poly-ubiquitin tag from the protein substrate in order to allow for translocation into the 20S core particle (20S CP) where the caspase, trypsin and chymotrypsin-like activities of the proteasome cleave it into small peptides for intracellular recycling [8–11]. This process is vital for proteostasis and defects in proteasome activity can be detrimental to cell survival.

### 1.1. Aggresomes

Cells have evolved several mechanisms to counteract transient decreases in proteolytic capacity. The aggresome pathway is one such mechanism and allows the cells to cope with increased proteotoxic stress following saturation of proteasome degradative capacity. In the event of insufficient proteasome activity, poly-ubiquitinated proteins form micro-aggregates that are trafficked along the microtubule network in a complex process involving, among others, HDAC6, VCP/p97

*Abbreviations:* ROS, Reactive oxygen species; SAHA, suberoylanilide hydroxamic acid; UPS, Ubiquitin-proteasome system; DUB, deubiquitinase; HDAC, Histone deacetylase; TRiC, TCP1-ring complex chaperonin; USP14, ubiquitin-specific protease 14; UCHL-5, Ubiquitin C-terminal hydrolase 5; RP, regulatory particle; CS, core particle; MTOC, microtubule organizing center; Hsp60, heat-shock protein 60; RNP, ribonucleoprotein Preprint submitted to Cancer Letters December 28, 2018

* Corresponding author. Department of Oncology-Pathology, Karolinska Institute, Stockholm, Sweden.
*E-mail address:* padraig.darcy@liu.se (P. D'Arcy).

https://doi.org/10.1016/j.canlet.2019.02.003
Received 8 November 2018; Received in revised form 28 December 2018; Accepted 1 February 2019

ATPase, p62/SQSTM1, and dynein. The proteins then aggregate as a single large inclusion body at the microtubule-organizing center (MTOC) [1,12–14]. This temporary accumulation of poly-ubiquitinated protein at the MTOC removes potentially harmful aggregates from the cytoplasm, effectively sequestering them [15,16], and is thought to be a phenomenon specifically associated with proteasome inhibition [17]. Aggresome formation facilitates the autophagic clearance of toxic protein aggregates in a p62-dependent manner [18], by creating a single location at which autophagic machinery can be positioned [19]. An autophagosomal membrane is then assembled around p62-positive aggregates in preparation for autophagic clearance [18,20]. Prolonged presence of aggresomes without autophagic clearance has been shown to lead to DNA damage and p53-mediated cell cycle arrest [21]. Aggresomes have recently been reported to be more dynamic structures than previously thought, and to exhibit ubiquitin-dependent liquid-like properties that allow for fission or fusion events to take place between aggregates [20,22], a process that may enable the formation of a single aggresome from multiple micro-aggregates. Consistent with the notion that the aggresome pathway is a protective mechanism, it has been found that agents which disrupt aggresome formation synergize with proteasome inhibitors in the induction of cytotoxicity [23–28]. As such, strategies that inhibit aggresome formation, to be used in combination with established proteasome inhibitors, are in various stages of development [29,30].

### 1.2. Current UPS inhibitors

The observation that malignant cells have a higher dependency on the UPS compared to normal cells provides a target for the rational design and development of selective therapies against cancer [31–34]. The approval of bortezomib for the treatment of multiple myeloma has verified the proteasome as a suitable target and stimulated interest in identifying the next generation of UPS inhibitors. An emerging problem with bortezomib-based regimes has been the development of acquired resistance [35,36]. Exactly how cells become resistant to proteasome inhibitor-based treatments is currently not known, although altered expression of proteasome catalytic subunits, especially PSMB5, and components of the heat shock response have been suggested to play a role [37–41]. To combat the problem of resistance to bortezomib, there has been a push to develop UPS inhibitors with targets other than the 20S catalytic subunit, and several such molecules have been the focus of recent publications [42–45].

### 1.3. DUB inhibitor b-AP15

We previously identified the small molecule b-AP15, a specific inhibitor of the proteasomal DUBs UCHL5 and USP14, that displays promising anti-tumor activity on a variety of solid and leukemic malignancies [46–51]. As b-AP15 is a non-catalytic proteasome inhibitor, with a different target site to bortezomib, this raises the possibility of combination therapies with conventional inhibitors in cases of acquired resistance. Exposure to b-AP15 induces the accumulation of poly-ubiquitinated protein, triggering a strong proteotoxic response associated with the production of ROS [52,53], ER stress [47,48,54], increased NK and T-cell mediated cancer cell death [50,55], and eventual apoptosis. Interestingly, the b-AP15-induced proteotoxic stress response does not lead to aggresome formation prior to cell death. Addition-ally, b-AP15 exposure alters the distribution and trafficking of mitochondria in the cytoplasm [56], indicating a broader effect on intracellular trafficking. Here we characterize the effects of b-AP15-induced proteotoxic stress on the aggresome response and intracellular transport, with the objective of determining a mechanism for b-AP15-dependent aggresome inhibition.

## 2. Materials and methods

### 2.1. Cell culture

HCT116 colon carcinoma cells were maintained in McCoy's 5A modified medium/10% FBS (fetal bovine serum) 100 units/mL penicillin, 100 µg/mL streptomycin. HeLa cells were cultured in DMEM medium supplemented with 10% FBS, 100 units/mL penicillin, 100 µg/mL streptomycin, and 4 mM L-glutamine. All cells were cultured at 37 °C and 5% CO2. The cell identity was confirmed by sequencing.

### 2.2. Immunofluorescence imaging

2 × 106 HCT116 and 1.2 × 105 HeLa cells were seeded on glass cover slips in 6-well plates and left to attach for 24 h. HCT116 cells were treated with 100 nM bortezomib and 1 µM b-AP15, and HeLa cells were treated with 1 µM bortezomib and 0.7 µM b-AP15 for indicated timepoints. Other inhibitors used: Mg132 (10 µM), p38IV (5 µM), Vinblastine (5 µM). For the combination treatment HeLa cells were pretreated for 4 h with vinblastine followed by the addition of 1 µM bortezomib and 0.7 µM b-AP15 for a further 12 h. Co-treatment with p38IV was carried out by adding the drugs simultaneously. After treatment cells were fixed in 4% formaldehyde (Merck) for 20 min at room temperature. Cells were permeabilized with 1% Triton X-100 (Sigma Aldrich) for 15 min in room temperature, followed by blocking with TBS/2% milk for 30 min in room temperature, and incubation with primary antibodies overnight at 4 °C. Primary antibodies used: p62 (BD 610833), K48-Ub (Millipore, 05-1307), Vimentin (Cell Signaling, 5741S), Ubiquitin (Santa Cruz, sc-8017) p97/VCP (Cell Signaling). To visualize cells by confocal microscope, cells were incubated with secondary antibody conjugated with fluorochromes for 1 h at room temperature. Secondary antibodies used: anti-mouse IgG FITC (Sigma Aldrich, F0257), anti-rabbit DyLight 594 (Vector, D1-1594), anti-mouse DyLight 594 (Vector, D1-2594), anti-rabbit DyLight 488 (Thermo Scientific, 35552). Cells were mounted using mounting media with DAPI (Vector, H-1500) and analyzed using a Leica confocal microscope or Zeiss Axiomanager 2 confocal microscope. Scoring of aggresome-positive cells was performed manually, representative images are presented. Colocalization analysis was performed using Pearson Cor-relation analysis in FIJI on n¿5 representative images per sample.

### 2.3. Electron microscopy

Cells were treated with b-AP15 for 12 h and fixed with 2.5% glutaraldehyde. Cells were post-fixed in 1% osmium tetraoxid, dehydrated and embedded in epoxy resin. Electron microscopy was performed as in Refs. [56,57].

### 2.4. His-Ubiquitin purification

6 × 105 HCT116 cells were transfected with 2 µg His-Ubiquitin and 1 µg of HDAC6 plasmid (Addgene 30482) [13] using FuGene6 transfection reagent. 24 h post transfection cells were treated with bortezomib (100 nM) or b-AP15 (1 µM) for an additional 6 h. Cells were collected by trypsinization and re-suspended in 1 mL of PBS. 65 µL of cell suspension was lysed directly in loading buffer as an input control. Remaining cells were centrifuged and lysed in 100 µl Buffer A (6 M Guanidine HCL, 0.1 M Na2HPO4/NaH2PO4), 10 mM imidazole, (pH 8) followed by sonication. 60 µl of a 50% slurry of Ni agarose was added and samples were incubated with rotation for 3 h at RT. Agarose was pelleted by centrifugation and washed/pelleted sequentially 2 X Buffer A, 2 X Buffer A/TI (1 vol Buffer A, 3 vol Buffer TI) and 1 X Buffer TI (25 mM Tris HCL, 20 mM Imidazole, pH 6.8). After the final wash pellet was re-suspended in loading buffer and run on SDS-PAGE gels. Ubiquitin-conjugated HDAC6 was detected using immunoblotting.

### 2.5. Polyubiquitin purification

Polyubiquitin interacting proteins were isolated using TUBE2 purification kit (Biosensors) according to manufacturer's protocol. In brief 5 × 106 cells were treated with DMSO, bortezomib or b-AP15 for 6 h and lysed in buffer (25 mM HEPES, 250 mM sucrose, 50 mM NaCl, 5 mM MgCl2, 2 mM ATP, supplemented with protease inhibitors). 25 µl TUBE2 agarose was added and samples incubated with rotation at 4 °C for 2 h. Samples were washed 3X with TBST, re-suspended in loading buffer and loaded on SDS-PAGE gels. Ubiquitin-protein interactions were detected by immunoblotting using specific antibodies.

### 2.6. Glycerol density gradient fractionation

Glycerol gradient fractionation of cell lysate was conducted on 15–35% linear glycerol gradients containing 25 mM Tris-HCl pH 7.6, 5 mM MgCl2, 1 mM dithiothreitol and 2 mM ATP. Cell lysates containing 500 µg of protein were loaded on glycerol gradients and samples were centrifuged at 26000 rpm for 28 h at 4 °C in an Optima L-80 XP Ultracentrifuge using a SW41 rotor (Beckman Coulter). Fractions were collected (24 × 500 µl) and proteins were precipitated in cold acetone for 1 h at −80 °C. Paired fractions were pooled and the 12 samples were prepared and used for immunoblotting.

### 2.7. Synergy experiments

HCT 116 cells were exposed to the indicated drug concentrations for 72 h. Viability was determined by MTT assay. The MacSynergy™ II program was used to calculate the efficiency of drug combinations in reducing cell viability (https://www.uab.edu/medicine/peds/macsynergy). The synergy plots generated by the MacSynergy™ II reflect the difference between experimentally determined results and the theoretical drug interactions, calculated from the dose response curves for each drug individually. The resulting plot appears as a flat surface for an additive effect, peaks indicate synergy and depressions indicate antagonism.

### 2.8. Mitochondrial isolation

Mitochondria were isolated using a mitochondria isolation kit (Sigma Aldrich MITOISO2). Of different protocols tested, this method was found to result in the lowest tubulin levels. Generally, 90% confluent cells in 20 cm dishes were collected by trypsinization and centrifuged for 5 min at 600 × *g*. Cell pellets were then resuspended in ice cold PBS and centrifuged again for 5 min at 600 × *g* at 2–8 °C and the supernatant discarded. Washing was repeated and 0.5 mL 1 x volume extraction buffer with cell lysis solution (1:200 v/v) was added to resuspend the cell pellet to a uniform suspension. Following incubation on ice for 5 min, 2 × 1 mL volume extraction buffer was added and the homogenate was centrifuged at 600 × *g* for 10 min at 4 °C. The supernatant was carefully transferred to a fresh tube followed by centrifugation at 11,000 × *g* for 10 min at 4 °C. Pellets were resuspended in ice cold PBS and centrifuged again for 5 min at 11,000 × *g*. The pellet was suspended in CelLytic M Cell Lysis Reagent with Protease Inhibitor Cocktail (1:100 [v/v]).

### 2.9. UbVS labeling

To assess effects of b-AP15 on DUBs, HCT116 cells were lysed by freeze-thawing 3x in lysis buffer (50 mM HEPES (pH 7.4), 250 mM sucrose, 10 mM MgC2, 2 mM ATP, 1 mM dithiothreitol). After removal of cell debris by centrifugation, total protein (25 mg, determined by Bradford Assay) was treated with indicated dosage of b-AP15 for 15 min at 37 °C and labeled with the active site probe UbVS (1 mM) for 30 min at 37 °C. Samples were visualized using SDS-PAGE and immunoblotting using specific USP14 (Millipore) and USP5 (Millipore), USP9x (Cell Signaling) and UCHL5 (Merck) antibodies.

### 2.10. Western Blot

Cells were lysed in UbVS lysis buffer (250 mM sucrose, 1 mM DTT, 5 mM MgCl2, 1 mM ATP, 50 mM Tris pH7.4). Cell debris was removed by centrifugation. Protein concentration was determined by Bradford assay, and protein levels were normalized before loading the lysates onto 4–12% SDS-PAGE/3–8% Tris-Acetate gels and separating them by electrophoresis. Proteins were transferred to nitrocellulose membranes and detected using specific antibodies: HDAC6 (Cell Signaling) K48-Ub (Millipore), p62, phospho-p62, phospho-p38, p38/MAPK13, PSMD14 (Cell Signaling).

### 2.11. Proteomics

Mitochondrial pellets were collected, washed 2x in PBS and lysed in 8M urea, 1% SDS, 50 mM Tris (pH 8.5) with protease inhibitors. Mitochondrial lysates were subjected to 1 min sonication on ice using Branson probe sonicator using 3 s on/off pulses with a 30% amplitude. Proteomics was then performed as in Ref. [56].

## 3. Results

### 3.1. b-AP15 induces poly-ubiquitin accumulation, has dominant-negative effect on aggresome formation

HeLa cells were treated with bortezomib or b-AP15 using an IC90 dose based on drug concentrations that induced maximal apoptosis after 24 h exposure. Already after 12 h exposure both bortezomib and b-AP15 induced the accumulation of K48-linked poly-ubiquitin in cells (Fig. 1a), consistent with reduced proteasome activity. These poly-ubiquitin aggregates co-localized with the ubiquitin-interacting chaperone p62/SQSTM1, a key mediator of aggresome formation and subsequent autophagic clearance [58].

Prolonged exposure to bortezomib (20 h) induced the formation of a single juxtanuclear poly-ubiquitin aggregate that co-localized with p62 in the majority of cells (≥60%) (Fig. 1a and b). Although b-AP15 induces similar, or even higher levels of poly-ubiquitin accumulation compared to bortezomib [46,56], b-AP15-treated cells failed to form characteristic aggresome structures. Instead the majority of b- AP15 treated cells displayed multiple poly-ubiquitin/p62 positive dots clustered in cytoplasmic and perinuclear regions (Fig. 1a and b). A similar result was obtained using HCT116 colon carcinoma cells (Supplementary Fig. 1) suggesting that the effect is not cell line-specific. The lack of distinct aggresome formation in cells exposed to b-AP15 is consistent with a recent report using several melanoma cell lines [51]. In confirmation of this observation, electron microscopy revealed the presence of a single electron-dense juxtanuclear aggregate in bortezomib-treated cells. In contrast, multiple aggregates that were scattered throughout the cytoplasm were observed in b-AP15-treated cells (Fig. 1c). To determine whether the effect of b-AP15 is dominant negative, we examined the results of co-treatment of HeLa cells with b-AP15 and bortezomib. Treatment with both drugs resulted in reduced aggresome formation compared to the effect observed when treating only with bortezomib (Fig. 1d).

We conclude that treatment with b-AP15 induces an atypical proteotoxic response that is not characterized by aggresome formation and exhibits a dominant-negative effect over bortezomib.

### 3.2. b-AP15 induces perinuclear vimentin clustering

Previous reports have shown that proteasome inhibition causes the re-localization of vimentin, a cytoskeletal type III intermediate filament, from the cytoplasm to the perinuclear region where it encases the nascent aggresome [12,59]. With this in mind we compared the effect

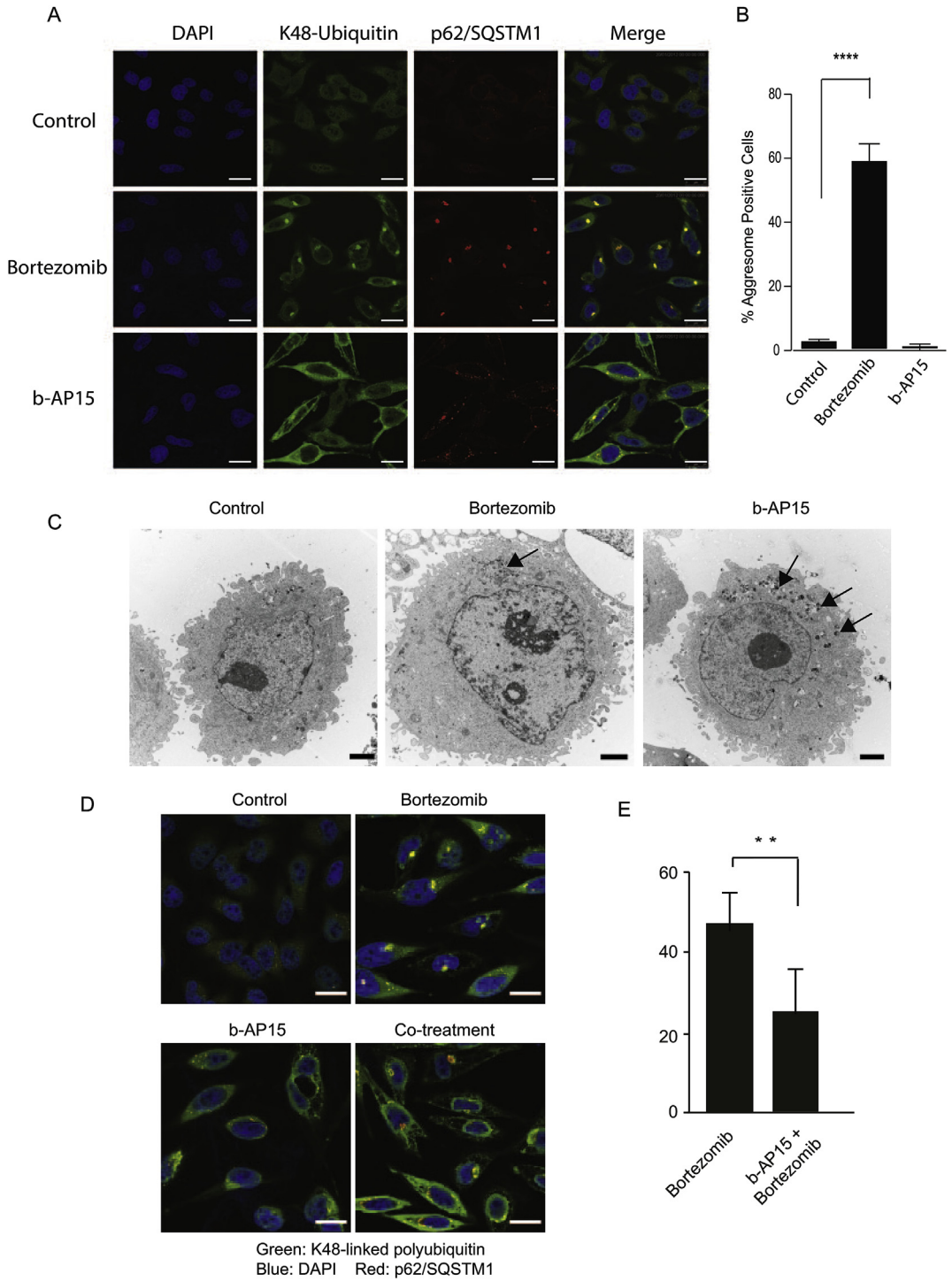


**Fig. 1.** A) HeLa cells treated with bortezomib or b-AP15 for 20 h. Aggresomes are visible and colocalized with p62/SQSTM1 for bortezomib, but no distinctive aggresome formation is visible in b-AP15-treated cells. B) Quantification of percentage of aggresome-positive cells after treatment with bortezomib or b-AP15 C) Electron micrograph of b-AP15 and bortezomib-treated cells showing a single juxtanuclear inclusion body of the aggresome in bortezomib-treated cells, but multiple smaller inclusion bodies scattered throughout the cytoplasm with b-AP15 treatment. D) Dominant negative effects of b-AP15 over bortezomib-induced aggresome formation in cells co-treated with both drugs. E) Bar-chart showing the reduction in percentage of aggresome-positive cells in response to co-treatment with bortezomib and b-AP15.

of bortezomib or b-AP15 treatment on vimentin localization. As shown in Fig. 2, both treatments resulted in the appearance of condensed vimentin localized in the perinuclear region (Fig. 2A). Treatment with Bortezomib resulted in more condensed and discrete vimentin clustering than b-AP15. Co-staining with ubiquitin antibodies showed the presence of vimentin cage structures surrounding a single ubiquitin positive locus in bortezomib-treated cells. In contrast, b-AP15 treated cells displayed condensed vimentin filaments interspersed with diffuse ubiquitin aggregates with no detectable vimentin cage structures (Fig. 2B). This data suggests that al-though both bortezomib and b-AP15 cause vimentin re-localization, the typical aggresome-associated vimentin-ubiquitin cage structures are absent in b-AP15 treated cells.

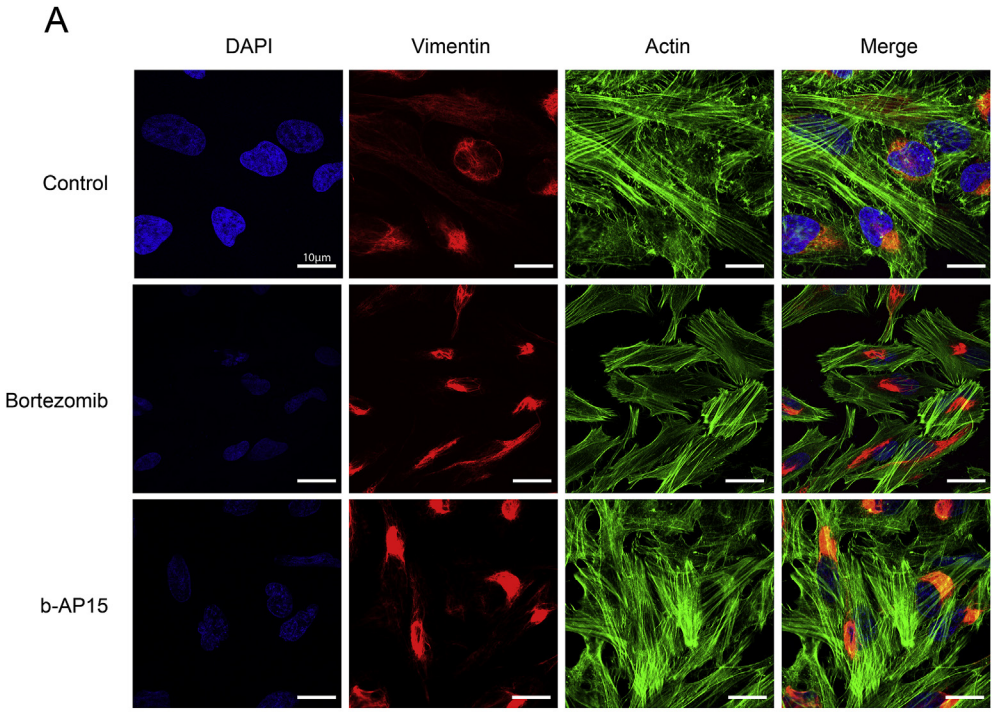


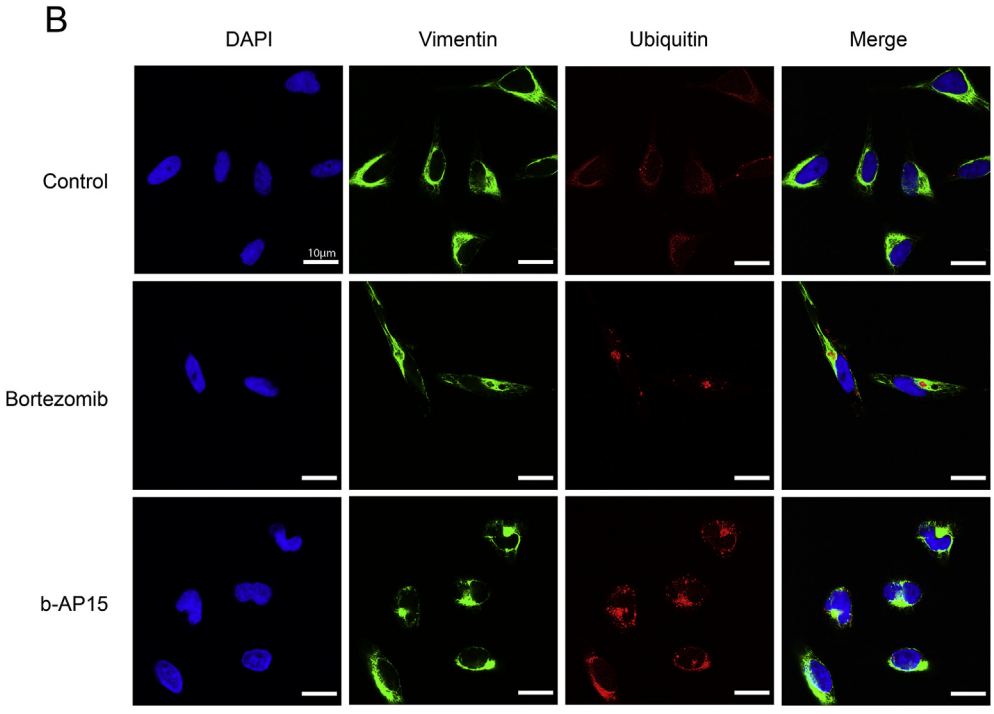


**Fig. 2.** HeLa cells were treated with bortezomib or b-AP15 for 20 h at $IC_{90}$ concentration. A) The distribution of vimentin and actin was visualized using fluorescent imaging. Bortezomib-treated cells displayed discrete perinuclear vimentin clusters, well separated from the surrounding actin skeleton. Treatment with b-AP15 also resulted in perinuclear vimentin clusters, but they appear more diffuse, and partially colocalize with the actin cytoskeleton. B) The distribution of K48-linked ubiquitin and the cytoskeletal intermediate protein vimentin was visualized using fluorescent imaging. Bortezomib treatment induced the formation of well-defined aggresomes, surrounded by characteristic vimentin cages. No aggresomes nor vimentin cages were formed in b-AP15-treated cells.

### *3.3. Poly-ubiquitin associates with the proteasome and components of the aggresome pathway*

A number of components are involved in the recognition of poly-ubiquitinated proteins by the 26S proteasome [60]. Glycerol gradient centrifugation showed that poly-ubiquitinated proteins are found associated with the proteasome in b-AP15 treated cells, indicating that b-AP15 does not interfere with the binding of poly-ubiquitinated substrates to the proteasome (Fig. 3a). Affinity purification of poly-ubiquitin chains from bortezomib- or b-AP15-treated cells showed the presence of the integral 19S subunit PSMD4/Rpn10 [61], consistent with continued poly-ubiquitin binding to the proteasome (Fig. 3b). Furthermore, we examined the interaction of affinity-purified poly-ubiquitinated proteins with other components of the aggresome pathway, such as the p97/VCP ATPase, involved in substrate processing [62], as well as p62/SQSTM1, a reported constituent of aggresomes, that has been suggested to play an essential role in protein micro-aggregate formation [20,63], and their subsequent trafficking to the aggresome [58]. Both these components were found to be associated with poly-ubiquitin chains to no lesser degree in treated cells (Fig. 3b).

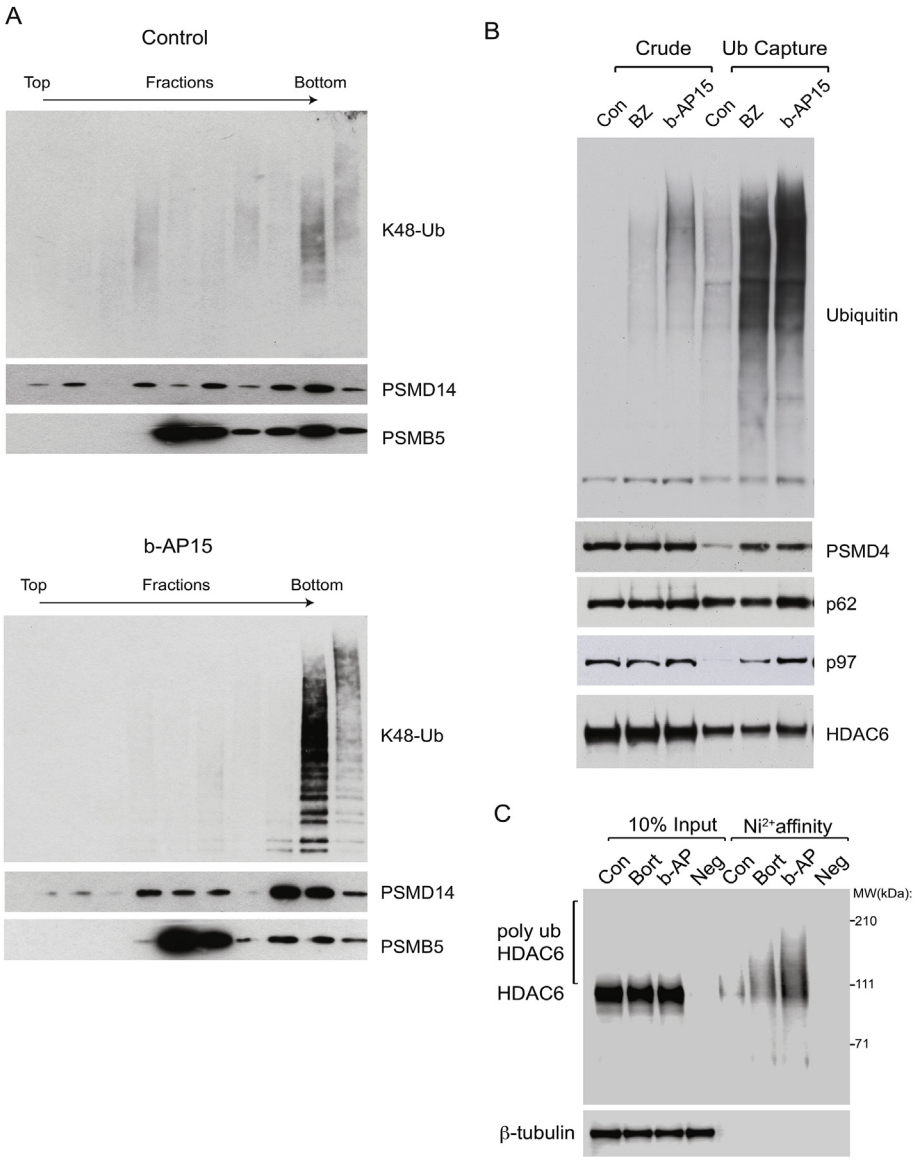


**Fig. 3.** A) Glycerol gradient centrifugation was performed to isolate the proteasomes, which segregate to the lower fractions as indicated by the presence of both 19S and 20S subunits. Proteasomes extracted from lysates of bAP15- treated cells showed increased accumulation of K48-linked poly-ubiquitin B) Ubiquitin-capture assay (TUBE) performed in HCT116 cells allowing for isolation of the various components of the aggresome machinery associated with poly-ubiquitin and visualization by Western Blot. C) Cells were transfected with His-Ubiquitin and a high-copy number plasmid of HDAC6. Following 6 h of treatment with bortezomib or b-AP15 poly-ubiquitin was isolated using Ni + affinity and HDAC6 levels detected by Western Blot, showing an increase in poly-ubiquitination of HDAC6.

Addition-ally, immunofluorescence imaging of HeLa cells treated with b-AP15 showed that p97/VCP ATPase is found to colocalize with the cytosolic clusters of poly-ubiquitin, just as in the aggresomes of bortezomib-treated cells (Supplemental Fig. 2). This suggests that chaperone-ubiquitin binding is not affected, and the aggresome machinery continues to be recruited to poly-ubiquitinated substrates.

During the process of aggresome formation, poly-ubiquitinated proteins are transported to the MTOC in complexes with histone deacetylase 6 (HDAC6), which is responsible for loading micro-aggregates onto dynein motor protein [13]. We found that HDAC6 was associated with poly-ubiquitin chains purified from b-AP15-treated cells (Fig. 3b). Additionally, a slight increase in HDAC6 ubiquitination was observed in affinity-purification of HDAC6 from those cells (Fig. 3c). This suggests that b-AP15 may inhibit DUBs involved in the regulation of HDAC6. However, the observed effect was weak and poly-ubiquitin smears were not observed in immunoblots of total lysates (Fig. 3b). Our data shows that bortezomib and b-AP15 induce a similar interaction of poly-ubiquitin with the aggresome machinery and the 26S proteasome.

### 3.4. Effects of b-AP15 on other aggresome pathway components

While the association of aggresome pathway components with poly-ubiquitin appeared unaffected by exposure to b-AP15, it is possible that b-AP15 has a direct or downstream effect on the activity of essential constituents of aggresome assembly. The tubulin disruptor vinblastine was used alone and in com-bination with Bortezomib to show that microtubule disruption in bortezomib-treated cells results in a phenotype resembling that of b-AP15-treated cells (Fig. 4a) However, clusters of polyubiquitin (red) remain associated with the p62/SQSTM1 (green). The multifunctional p62 protein plays a central role in the formation of both micro-aggregates and aggresomes [22,58], as well as linking the UPS to autophagic clearance pathways. In order for p62 to actively bind and aggregate poly-ubiquitinated proteins it must be phosphorylated at Thr269/Ser272 by MAPK p38. The p38 enzyme is in turn activated in response to proteotoxic stress [22,64]. To determine the activity of these aggresome pathway components we tested the protein levels and phosphorylation levels of p38/MAPK13 and p62/SQSTM1 in cells treated with b-AP15, bortezomib or the generic proteasome inhibitor MG132 (Fig. 4c). After 6 h of exposure, expression levels of p38 and p62 remain essentially unchanged, and only control cells display phosphorylation of p38. Protein levels of p38 do not change even after 21 h of treatment, however, b-AP15 exposure induces p38 phosphorylation, and a strong increase in p62 phosphorylation at Thr269/Ser272, consistent with its activation by p38. There is also an observable increase in

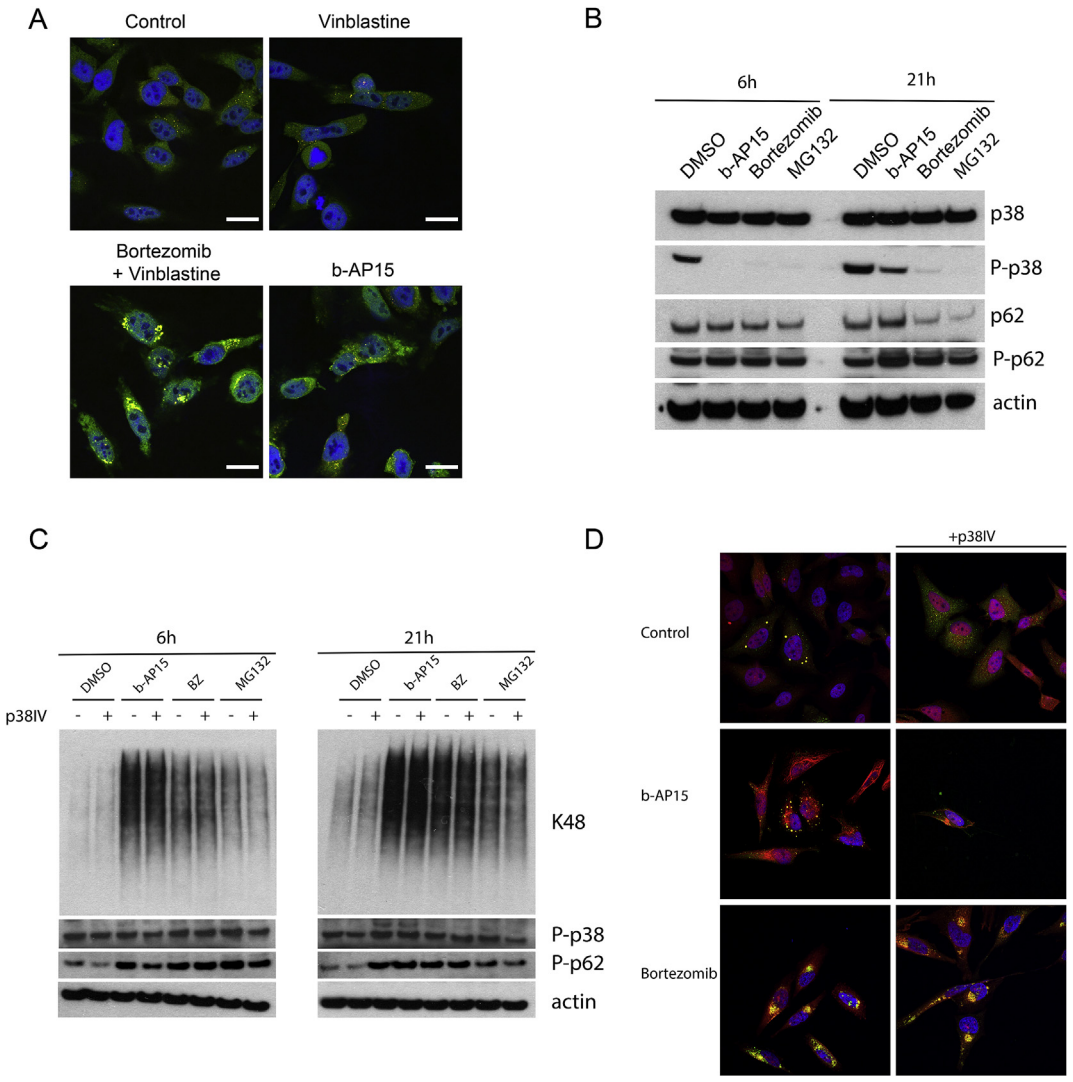


**Fig. 4.** A) HeLa cells were pre-treated for 4 h with 5 μM vinblastine, followed by additional treatment with bortezomib for 12 h, or single treatment with b-AP15. Aggresomes were visualized using K48-ubiquitin (red) and p62/SQSTM1 (green) primary antibodies. Vinblastine pre-treatment abrogated aggresome formation in bortezomib-treated cells. K48-ubiquitin and p62/SQSTM1 are colocalized in both b-AP15-treated cells and those exposed to a combination of vinblastine and bortezomib. B) Western Blot analysis of the levels of p38, phospho-p38, p62/SQSTM1 and phospho-p62 (Thr269/Ser272) in cells treated with 0.7 μM b-AP15, 1 μM Bortezomib and 10 μM MG132 for the indicated times. No effects were visible for either treatment after 6 h. After 21 h, only b-AP15 treatment resulted in an increase in p62 levels, as well as an increase in phosphorylated p38, and a strong increase in p62 phosphorylated at the Thr269/Ser272 position, indicating its activation by p38. C) Effects of the p38 inhibitor p38IV on p38 and p62 activation in combination with b-AP15, bortezomib and MG132. Th inhibitor had no visible effect on p38 phosphorylation, but resulted in a marked increase in downstream p62 phosphorylation at Thr269/Ser272. However, at the late timepoint, p62 is phosphorylated despite the presence of p38IV, suggesting alternative methods of p62 activation. D) Confocal imaging of aggresome formation in the presence of p38IV. After 21 h of treatment, p38 inhibition did not interfere with aggresome formation in bortezomib-treated cells. No alteration in ubiquitin distribution was observed in cells co-treated with b-AP15 and p38IV. However, the co-treatment may have resulted in an accelerated onset of apoptosis. (For interpretation of the references to colour in this figure legend, the reader is referred to the Web version of this article.)

p62 protein levels after 21 h of b-AP15 treatment, suggesting that proteotoxic stress due to pro-longed b-AP15 exposure leads to elevated p62 levels, whereas proteasome inhibition by bortezomib and MG132 does not. We also tested whether inhibiting p38 activity would prevent aggresome formation in bortezomib-treated cells, or dis-play additional effects in combination with b-AP15 (Fig. 4c and d). Inhibition of p38 using the p38IV inhibitor resulted in no reduction of p38 phosphorylation, but a marked decrease in p62 phosphorylation at Thr269/Ser272, indicating successful p38 inhibition. Treatment with b-AP15 did not reduce p62 nor p38 phosphorylation, suggesting that b-AP15 does not prevent aggresome formation by interfering with the mechanism of micro-aggregate formation, and acts further downstream (Fig. 4c). Confocal microscopy of cells treated with b-AP15 and p38IV showed no alteration in ubiquitin distribution. Furthermore, p38IV did not prevent aggresome formation in bortezomib-treated cells (Fig. 4d). This, together with the increase in p62 phosphorylation at the 21 h timepoints in 4c, observed with b-AP15, Bortezomib and MG132, despite the presence of p38IV, suggests a redundant mechanism of p62 activation that functions as an alternative to p38-dependent p62 phosphorylation. Additionally it has previously been reported that the inhibition of USP9x, a multifunctional DUB, by the small-molecule WP-1130 is a potent inducer of aggresome formation [44]. Another DUB, USP5, is also targeted by WP-1130, and is involved in maintaining the cellular pool of unanchored polyubiquitin. We therefore tested the effects of b-AP15 on USP9x and USP5 activity, using the DUB active-site probe UbVS (ubiquitin-vinylsulfone). We also included the known b-AP15 tar-get USP14 and the other proteasome associated DUB UCHL5. (Supplemental Fig. 3). Treatment with b-AP15 showed no effect on

USP9X activity, nor on the activity of the USP5 DUB. Inhibition was only observed for USP14.

### 3.5. b-AP15 treatment has no visible effects on tubulin network

Tubulin inhibitors have been shown to abrogate aggresome formation by disrupting the traffic of ubiquitinated cargo to the MTOC region [12,59]. As shown in Fig. 4a, co-treatment of HeLa cells with vinblastine blocked bortezomib-induced aggresome formation, resulting in the appearance of predominantly cytoplasmic polyubiquitin aggregates lacking typical aggresome structure. The inhibition of effective trafficking of poly-ubiquitinated cargo to the aggresome suggested a possible effect on the microtubule network itself. Confocal microscopy of cells treated with b-AP15 or bortezomib indicated however that microtubules remained intact and largely unaffected by treatment with both b-AP15 and bortezomib (Supplemental Fig. 4a) and remained stable for both early (6 h) and late (21 h) timepoints (Supplemental Fig. 4b).

### 3.6. Transport of clathrin-coated vesicles is affected by b-AP15 at late timepoints

Clathrin-mediated endocytosis and the transport of Clathrin-coated vesicles is generally accepted to be largely dependent on the actin cytoskeleton [90,91]. No obvious redistribution of clathrin was observed in b-AP15-treated cells at the early timepoint (6 h). However, the later timepoint (18 h) indicated an increase in the accumulation of clathrin in the perinuclear region (Supp. Fig.5a). This may indicate a defect in anterograde transport of vesicles from the Golgi towards the cell periphery. The effects of b-AP15 on the actin cytoskeleton were also examined using phalloidin staining (Supp. Fig. 5b). As before, there is no discernible effect on the actin network at the early timepoint, while after 18 h of treatment, there is evidence of intracellular actin accumulation at the nuclear periphery.

### 3.7. Absence of aggresomes not due to inhibition of HDAC6 tubulin deacetylation activity

HDAC6 regulates aggresome formation in part due to its ability to deacetylate tubulin [65]. Abrogation of HDAC6 function, either through siRNA knock-down or chemical inhibition, is known to block aggresome formation and result in the accumulation of multiple polyubiquitin complexes in the cytoplasm and increased proteotoxicity [13,15,23]. We considered the possibility that the weak increase in ubiquitination (Fig. 3c) altered HDAC6 function and tubulin acetylation levels. The effect of bortezomib and b-AP15 on tubulin acetylation was compared, with the pan-HDAC inhibitor suberoylanilide hydroxamic acid (SAHA). SAHA is known to inhibit aggresome formation and to induce synergism with bortezomib in cell survival assays [66–68]. No increase in tubulin acetylation was observed in cells exposed to b-AP15 or bortezomib (Fig. 5a and b). Using HCT cells in cell-survival based assays we were able to show a synergystic effect using bortezomib and SAHA in combination (Fig. 5c). In contrast, b-AP15 showed no synergy with SAHA (Fig. 5c) indicating that b-AP15 effectively induces proteotoxicity on its own, not requiring adjuvant treatment.

### 3.8. Alteration in mitochondrial localization suggests effect on microtubule-dependent transport

The lack of obvious changes in microtubuli structure does not preclude the possibility of changes in tubulin dynamics or in the kinesin/dynein systems. Such alterations would explain the low degree of aggresome formation in b-AP15-treated cells and would be consistent with the findings in Fig. 4a. Similar to aggresomes, mitochondria and other organelles are known to be transported in cells by microtubule-based transport via kinesin and dynein motors [69–72]. We examined the distribution of mitochondria in b-AP15- treated cells using immunostaining for Hsp60. Even at the early timepoint of 6 h, prior to the induction of apoptosis and any morphological changes, we observed a redistribution of mitochondria to perinuclear areas (Fig. 6a).

Mitochondrial Rho GTPases are known to couple mitochondria to the tubulin system [69]. Analysis by mass spectrometry did not show any decreases in mitochondrial Rho1/Miro1 or mitochondrial Rho2/Miro2 in isolated mitochondria prepared from b-AP15-treated cells (Fig. 6b). However, the levels of other proteins were found to be altered. Of the 20 proteins that showed the greatest increase in mitochondrial fractions after b-AP15 treatment, five were related to RNA processing (DCP1A, EDC3, EDC4, DDX6 and PATL1), and known to be associated with P-bodies [73–76] (Fig. 6c). These are subcellular ribonucleoprotein (RNP) granules that are linked to the micro-tubule network and are known to be trafficked by dynein/kinesin motor proteins [76–78]. We also observed increases in several constituents of the centrosome (SSX2IP, MIB1, PCM1, CEP131, OFD1, PIBF1, and AKAP9) (Fig. 6c) [79–85]. These findings are consistent with drug-induced impairment of organelle transport, resulting in colocalization of P-bodies and mitochondria in the vicinity of centrosomes. Among the proteins that decreased most dramatically in mitochondrial fractions were chaperonin II proteins associated with TRiC/CCT (Fig. 6d) [86–88]. TRiC/CCT proteins are known to be involved in the maintenance of a pool of α/β-tubulin heterodimers [89]. Tubulin levels in mitochondrial fractions were, however, not affected (Fig. 6b).

## 4. Discussion

b-AP15 is a bis-benzylidine piperidone compound containing α, β-unsaturated carbonyl functionalities. The cellular response to b-AP15 is characteristic of proteasome inhibitors [48,92]. Apoptosis induction by b-AP15 and similar drugs is not affected by overexpression of Bcl-2 [46,93]. We and others have reported that b-AP15 and similar molecules [43] induces a higher level of proteotoxic stress than observed with bortezomib [52,56,94].

Here we show that unlike other proteasome inhibitors, b-AP15 does not induce aggresome formation in HeLa cells (Fig. 1a). Similar results were observed in A549 and HCT116 cells, and are in agreement with a recent observation in melanoma cells [51]. We found that b-AP15 inhibited bortezomib-induced aggresome formation, showing that the effect of b-AP15 is dominant negative (Fig. 1d). The effect on aggresome formation is of interest from a drug development perspective, since the lack of aggresomes indicates a disruption of a potential survival mechanism and is therefore an attractive feature of this class of drugs. It is well established in the literature that the antiproliferative effect of bortezomib is enhanced by the histone deacetylase inhibitor SAHA [24,25,66–68,95]. We here show that, in contrast to bortezomib, the cytotoxic effect of b-AP15 is additive, but not synergistic with SAHA treatment.

We have previously demonstrated re-localization of poly-ubiquitinated protein to the outer membranes of mitochondria [56], in response the b-AP15 treatment, possibly resulting in mitochondrial damage and apoptosis. The lack of aggresome formation following b-AP15 treatment may explain these observations. Interestingly the inhibitory effect of b-AP15 on the aggresome pathway seems to be specific, since other DUB inhibitors seem to enhance rather than inhibit aggresome formation. WP-1130, a recently described DUB inhibitor, has been shown to inhibit the activities of USP5, USP9X, UCHL1 as well as the proteasomal DUBs, UCHL5 and USP14 [44]. Although WP-1130 induced polyubiquitin accumulation similar to b-AP15, it was also a potent inducer of aggresome formation, with characteristic aggresome structures detectable after only 4 h of WP-1130 exposure. These rapid kinetics of aggresome formation surpass that of conventional 20S inhibitors such as MG132 and bortezomib, which generally require treatment times over 12 h. A second more broad range DUB inhibitor, PR-619 also induced the formation of aggresome complexes enriched

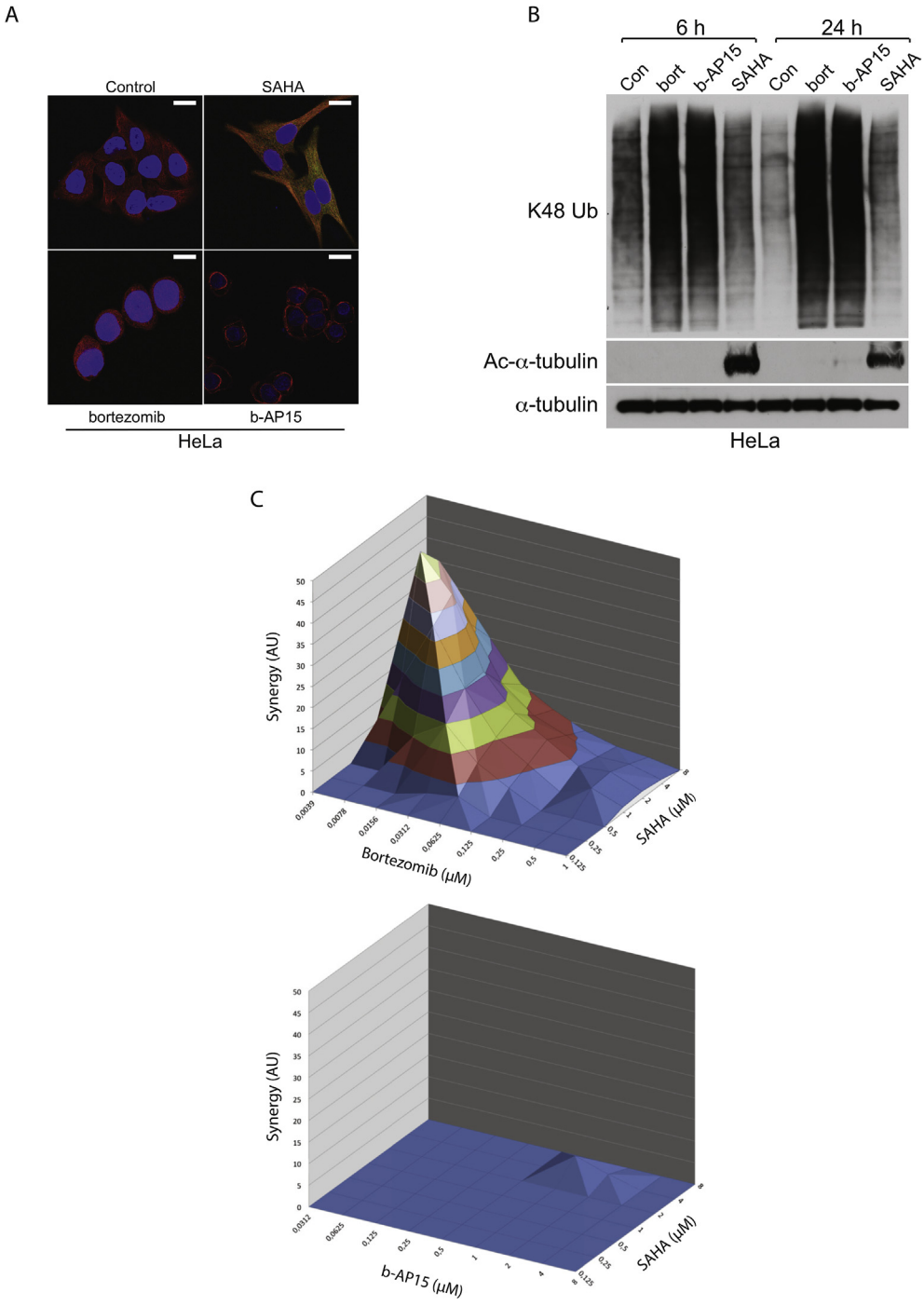


**Fig. 5.** A) HeLa cells were treated with the pan-HDAC inhibitor SAHA, bortezomib, or b-AP15 (20 h), and tubulin (red) and tubulin acetylation (green) were detected using specific antibodies. B) Western Blot analysis of lysates of bortezomib-, b-AP15-, and SAHA-treated cells, showing no increase in acteyl-tubulin with bortezomib or b-AP15, and no effect on total α-tubulin levels at 6 h or 24 h. C) A cell survival-based assay showing synergistic effects between bortezomib and SAHA, but no synergy when combining treatment with b-AP15. The synergy plots reflect the difference between experimentally determined results and the predicted drug interactions, calculated from the dose response curves for each drug. The resulting plot appears as a flat surface for an additive effect, peaks indicate synergy and depressions indicate antagonism. (For interpretation of the references to colour in this figure legend, the reader is referred to the Web version of this article.)

with ubiquitin, p62 and HSP70 [96]. These observations suggest that aggresome formation may in part be regulated by the activity of specific DUBs, particularly USP14 or UCHL5, or the observed inhibition may be due to a specific off-target effect by b-AP15.

It is important to realize, however, that the precise mechanism of action is likely to be complex due to potential thiol-reactivity of b-AP15. We have therefore not attempted to determine the exact mechanism of b-AP15-induced aggresome inhibition, since it is likely to involve more than one pathway. Furthermore, a recent siRNA screen showed that at least 29 different proteins were of mechanistic importance for aggresome formation [97], providing a broad range of potential targets. We do show that poly-ubiquitinated substrates dock to the proteasome and are associated with p97/VCP, p62 and HDAC6. We also see colocalization of poly-ubiquitin and p97/VCP as well as p62 in the cytosol. Treatment with b-AP15 does not prevent p62 phosphorylation, nor inhibit its activity in micro-aggregate formation (Fig. 4), indicating that the defect occurs in trafficking, rather than the assembly of the aggresome machinery. We have also shown that b-AP15 has no inhibitory effect USP9X and USP5, the other DUBs known to be involved in aggresome formation.

Previous research has shown that b-AP15 has an effect on mitochondrial distribution and trafficking [56], suggesting a broader impact of b-AP15 on intracellular traffic. We show here that mitochondria re-localize to the perinuclear region in b-AP15-treated cells and become associated with P-bodies. Both of these structures are known to be transported by kinesin/dynein motors [76–78]. We also found centrosomal proteins associated with mitochondria, and observed a simultaneous loss of several proteins associated with the cytosolic

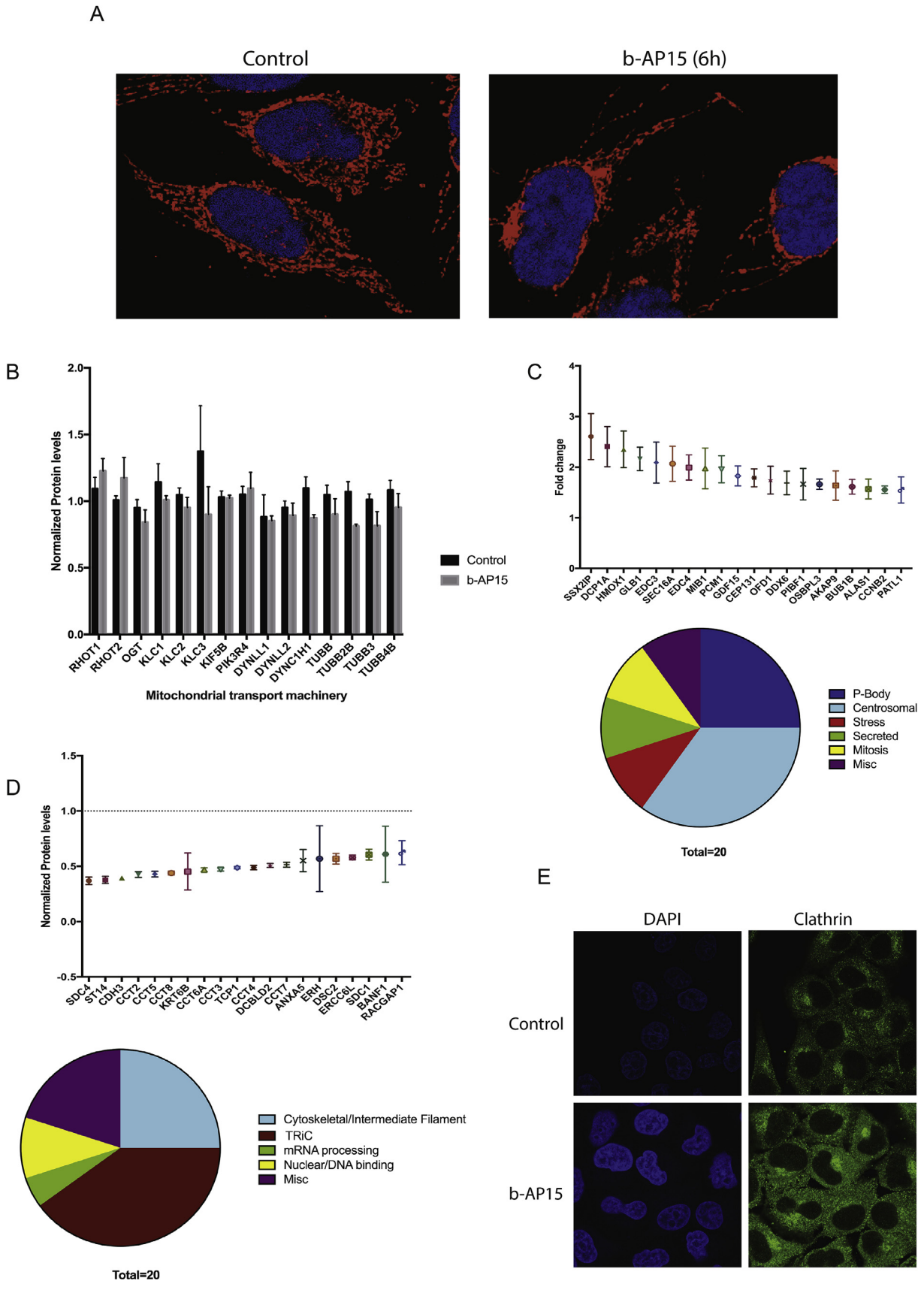


*(caption on next page)*

**Fig. 6.** A) Cellular localization of mitochondria in untreated cells and after 6 h of exposure to b-AP15, showing collapse of typical mitochondrial distribution and accumulation in the nuclear periphery. B) Normalized protein levels of canonical mitochondrial transport machinery, as well as tubulins, found associated with mitochondria in b-AP15 treated cells. All changes were non-significant. C) 20 proteins displaying the greatest increase in accumulation on mitochondria in response to b-AP15 treatment compared to untreated control. The pie chart shows the proportion of those 20 proteins typically associated with P-bodies, the centrosome, cellular stress, secretion, mitosis or other. D) 20 proteins displaying the greatest decrease in protein levels found on isolate mitochondria in response to b-AP15 treatment. The pie chart shows the pro-portion of those proteins typically found in the cytoskeleton, TRiC (TCP1-ring complex chaperonin), cell membrane, nucleus, mRNA processing, or other.

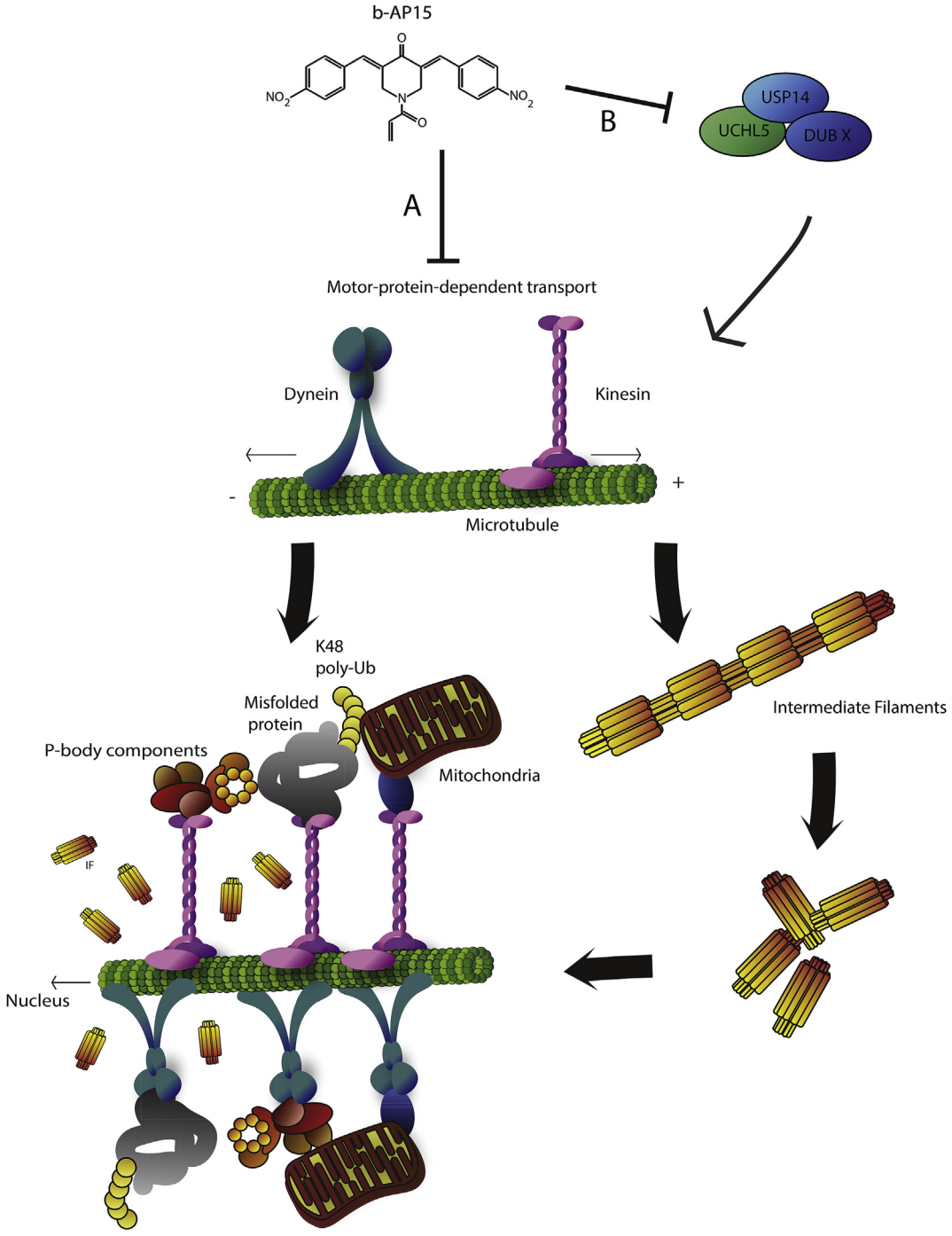


**Fig. 7.** A graphical outline of the potential modes of b-AP14 action of the aggresome formation pathway. A) b-AP15 acts on motor protein dependent transport by interfering directly or indirectly with dynein and kinesin motor protein function or B) b-AP15-dependent inhibition of DUBs interferes with motor protein function. Both modes lead to inhibition of intracellular transport machinery, resulting in impaired aggresome formation, mitochondrial damage, and enhanced cytotoxicity.

components of the intermediate filament network [98] from the mitochondrial surface. Furthermore, transport of the intermediate filament vimentin, which is known to be trafficked and organized in a motor protein-dependent manner along microtubules [99,100], is similarly affected by exposure to b-AP15 and displays perinuclear clustering (Fig. 2). Vimentin is known to stabilize intracellular mechanics and organelle localization, and frequently aligns with microtubules in a kinesin-dependent manner [101,102]. Our data suggest effects downstream from the proteasome, at the level of cargo transport by the kinesin/dynein system. Our interpretation of these results is that the dynamics of the microtubule transport system are affected by b-AP15, resulting in defects in aggresome formation and the impairment of motor protein-dependent cargo transport.

Since b-AP15 appears to inhibit intracellular trafficking of various substrates, an off-target effect on cellular transport machinery is possible. Whether this effect is exerted directly by b-AP15 targeting of transport components, such as kinesin and dynein, or by indirect action via inhibition of regulatory DUBs that deubiquitinate transport machinery warrants further study. In Fig. 7 we show the potential pathways for b-AP15 action on motor protein-dependent transport, and the resulting accumulation of protein aggregates, mitochondria, and P-bodies in close proximity to one another. This prevents effective sequestration of toxic misfolded protein from the cytoplasm, and ultimately leads to the increased proteotoxicity observed with b-AP15 treatment, making it an at-tractive option in cancer treatment, since it does not require the use of adjuvant treatment to enhance its proteotoxic effects.

## Conflicts of interest

All authors declare that they have no conflict of interest with the contents of this study.

## Acknowledgement

We are grateful to Radiumhemmets Forskningsfonder (grant number: 154193), Cancerfonden (grant number: 15 0818), Vetenskapsrådet (2015-02905), Barncancerfonden (2015-0091) and Knut och Alice Wallenbergs Stiftelse (2015.0063) for the funding that financed this project. Additional thanks are due to C Triola for helpful comments and discussion.

## Appendix A. Supplementary data

Supplementary data to this article can be found online at https://doi.org/10.1016/j.canlet.2019.02.003.

## References

[1] R.R. Kopito, Aggresomes, inclusion bodies and protein aggregation, Trends Cell Biol. 10 (12) (2000) 524–530.
[2] R. Wetzel, Mutations and off-pathway aggregation of proteins, Trends Biotechnol. 12 (5) (1994) 193–198.
[3] A.L. Fink, Protein aggregation: folding aggregates, inclusion bodies and amyloid, Fold. Des. 3 (1) (1998) R9.
[4] K.L. Rock, C. Gramm, L. Rothstein, K. Clark, R. Stein, L. Dick, D. Hwang, A.L. Goldberg, Inhibitors of the proteasome block the degradation of most cell proteins and the generation of peptides presented on MHC class I molecules, Cell 78 (5) (1994) 761–771.
[5] A. Borodovsky, B.M. Kessler, R. Casagrande, H.S. Overkleeft, K.D. Wilkinson, H.L. Ploegh, A novel active site-directed probe specific for deubiquitylating enzymes reveals proteasome association of USP14, EMBO J. 20 (18) (2001) 5187–5196.
[6] M. Hu, P. Li, L. Song, P.D. Jeffrey, T.A. Chernova, K.D. Wilkinson, R.E. Cohen, Y. Shi, Structure and mechanisms of the proteasome-associated deubiquitinating enzyme USP14, EMBO J. 24 (21) (2005) 3747–3756.
[7] A. Guterman, M.H. Glickman, Complementary roles for Rpn11 and UBP6 in deubiquitination and proteolysis by the proteasome, J. Biol. Chem. 279 (3) (2003) 1729–1738.
[8] K. Tanaka, The proteasome: overview of structure and functions, Proc. Jpn. Acad. B 85 (1) (2009) 12–36.
[9] M. Rechsteiner, L. Hoffman, W. Dubiel, The multicatalytic and 26S proteases, J. Biol. Chem. 268 (9) (1993) 6065–6068.
[10] Y.A. Lam, W. Xu, G.N. DeMartino, R.E. Cohen, Editing of ubiquitin conjugates by an isopeptidase in the 26S proteasome, Nature 385 (6618) (1997) 737–740.
[11] A. Hershko, A. Ciechanover, A. Varshavsky, The ubiquitin system, Nat. Med. 6 (10) (2000) 1073.
[12] J.A. Johnston, C.L. Ward, R.R. Kopito, Aggresomes: a cellular response to misfolded proteins, J. Cell Biol. 143 (7) (1998) 1883–1898.
[13] Y. Kawaguchi, J.J. Kovacs, A. McLaurin, J.M. Vance, A. Ito, T.P. Yao, The deacetylase HDAC6 regulates aggresome formation and cell viability in response to misfolded protein stress, Cell 115 (6) (2003) 727–738.
[14] C. Boyault, B. Gilquin, Y. Zhang, V. Rybin, E. Garman, W. Meyer-Klaucke, P. Matthias, C.W. Müller, S. Khochbin, HDAC6—p97/VCP controlled polyubiquitin chain turnover, EMBO J. 25 (14) (2006) 3357–3366.
[15] A. Rodriguez-Gonzalez, T. Lin, A.K. Ikeda, T. Simms-Waldrip, C. Fu, K.M. Sakamoto, Role of the aggresome pathway in cancer: targeting histone deacetylase 6–dependent protein degradation, Cancer Res. 68 (8) (2008) 2557–2560.
[16] N. Zaarur, A.B. Meriin, V.L. Gabai, M.Y. Sherman, Triggering aggresome formation: dissecting aggresome-targeting and aggregation signals in syphilin 1, J. Biol. Chem. 283 (41) (2008) 27575–27584.
[17] J. Szeto, N.A. Kaniuk, V. Canadien, R. Nisman, N. Mizushima, T. Yoshimori, D.P. Bazett-Jones, J.H. Brumell, ALIS are stress-induced protein storage compartments for substrates of the proteasome and autophagy, Autophagy 2 (3) (2006) 189–199.
[18] P. Sanchez-Martin, M. Komatsu, p62/SQSTM1—steering the cell through health and disease, J. Cell Sci. 131 (21) (2018) JCS222836.
[19] N. Zaarur, A.B. Meriin, E. Bejarano, X. Xu, V.L. Gabai, A.M. Cuervo, M.Y. Sherman, Proteasome failure promotes positioning of lysosomes around aggresome via local block of microtubule-dependent transport, Mol. Cell Biol. 34 (7) (2014) 1336–1348.
[20] G. Zaffagnini, A. Savova, A. Danieli, J. Romanov, S. Tremel, M. Ebner, T. Peterbauer, M. Sztacho, R. Trapannone, A.K. Tarafder, et al., p62 filaments capture and present ubiquitinated cargos for autophagy, EMBO J. (2018) e98308.
[21] M. Lu, C. Boschetti, A. Tunnacliffe, Long term aggresome accumulation leads to DNA damage, p53-dependent cell cycle arrest, and steric interference in mitosis, J. Biol. Chem. 290 (46) (2015) 27986–28000.
[22] D. Sun, R. Wu, J. Zheng, P. Li, L. Yu, Polyubiquitin chain-induced p62 phase separation drives autophagic cargo segregation, Cell Res. 1 (2018).
[23] S.T. Nawrocki, J.S. Carew, M.S. Pino, R.A. Highshaw, R.H. Andtbacka, K. Dunner, A. Pal, W.G. Bornmann, P.J. Chiao, P. Huang, et al., Aggresome disruption: a novel strategy to enhance bortezomib-induced apoptosis in pancreatic cancer cells, Cancer Res. 66 (7) (2006) 3773–3781.
[24] T. Hideshima, J.E. Bradner, J. Wong, D. Chauhan, P. Richardson, S.L. Schreiber, K.C. Anderson, Small-molecule inhibition of proteasome and aggresome function induces synergistic antitumor activity in multiple myeloma, Proc. Natl. Acad. Sci. 102 (24) (2005) 8567–8572.
[25] L. Catley, E. Weisberg, T. Kiziltepe, Y.T. Tai, T. Hideshima, P. Neri, P. Tassone, P. Atadja, D. Chauhan, N.C. Munshi, et al., Aggresome induction by proteasome inhibitor bortezomib and α-tubulin hyperacetylation by tubulin deacetylase (TDAC) inhibitor LBH589 are synergistic in myeloma cells, Blood 108 (10) (2006) 3441–3449.
[26] D.T. Vogl, P.N. Hari, S. Jagannath, S.S. Jones, J.G. Supko, G. Leone, C. Wheeler, R.Z. Orlowski, P.G. Richardson, S. Lonial, ACY-1215, a selective histone deacetylase (HDAC) 6 inhibitor: interim results of combination therapy with bortezomib in patients with multiple myeloma (MM), Blood 122 (21) (2013) 759.
[27] P.G. Richardson, C.S. Mitsiades, J.P. Laubach, R. Hajek, I. Spicka, M.A. Dimopoulos, P. Moreau, D.S. Siegel, S. Jagannath, K.C. Anderson, Preclinical data and early clinical experience supporting the use of histone deacetylase inhibitors in multiple myeloma, Leuk. Res. 37 (7) (2013) 829–837.
[28] D.J. McConkey, M. White, W. Yan, erHDAC inhibitor modulation of pro- teotoxicity as a therapeutic approach in cancer, Adv. Canc. Res. 116 (2012) 131–163 Elsevier.
[29] S. Komatsu, S. Moriya, X.F. Che, T. Yokoyama, N. Kohno, K. Miyazawa, Combined treatment with SAHA, bortezomib, and clarithromycin for concomitant targeting of aggresome formation and intracellular proteolytic pathways enhances ER stress-mediated cell death in breast cancer cells, Biochem. Biophys. Res. Commun. 437 (1) (2013) 41–47.
[30] S. Moriya, S. Komatsu, K. Yamasaki, Y. Kawai, H. Kokuba, A. Hirota, X.F. Che, M. Inazu, A. Gotoh, M. Hiramoto, et al., Targeting the integrated networks of aggresome formation, proteasome, and autophagy potentiates ER stress-mediated cell death in multiple myeloma cells, Int. J. Oncol. 46 (2) (2015) 474–486.
[31] R.Z. Orlowski, D.J. Kuhn, Proteasome inhibitors in cancer therapy: lessons from the first decade, Clin. Cancer Res. 14 (6) (2008) 1649–1657.
[32] L.J. Crawford, B. Walker, A.E. Irvine, Proteasome inhibitors in cancer therapy, J. Cell Commun. Signal 5 (2) (2011) 101–110.
[33] R.J. Deshaies, Proteotoxic crisis, the ubiquitin-proteasome system, and cancer therapy, BMC Biol. 12 (1) (2014) 94.
[34] E.E. Manasanch, R.Z. Orlowski, Proteasome inhibitors in cancer therapy, Nat. Rev. Clin. Oncol. 14 (7) (2017) 417.
[35] P.G. Richardson, B. Barlogie, J. Berenson, S. Singhal, S. Jagannath, D. Irwin, S.V. Rajkumar, G. Srkalovic, M. Alsina, R. Alexanian, et al., A phase 2 study of bortezomib in relapsed, refractory myeloma, N. Engl. J. Med. 348 (26) (2003) 2609–2617.
[36] S. Lonial, E.K. Waller, P.G. Richardson, S. Jagannath, R.Z. Orlowski, C.R. Giver, D.L. Jaye, D. Francis, S. Giusti, C. Torre, et al., Risk factors and kinetics of

thrombocytopenia associated with bortezomib for relapsed, refractory multiple myeloma, Blood 106 (12) (2005) 3777–3784.
[37] D. Chauhan, G. Li, R. Shringarpure, K. Podar, Y. Ohtake, T. Hideshima, K.C. Anderson, Blockade of Hsp27 overcomes bortezomib/proteasome inhibitor PS-341 resistance in lymphoma cells, Cancer Res. 63 (19) (2003) 6174–6177.
[38] R. Oerlemans, N.E. Franke, Y.G. Assaraf, J. Cloos, I. van Zantwijk, C.R. Berkers, G.L. Scheffer, K. Debipersad, K. Vojtekova, C. Lemos, et al., Molecular basis of bortezomib resistance: proteasome subunit β5 (PSMB5) gene mutation and overexpression of PSMB5 protein, Blood 112 (6) (2008) 2489–2499.
[39] S. Lü, J. Yang, Z. Chen, S. Gong, H. Zhou, X. Xu, J. Wang, Different mu- tants of PSMB5 confer varying bortezomib resistance in T-lymphoblastic lymphoma/leukemia cells derived from the Jurkat cell line, Exp. Hematol. 37 (7) (2009) 831–837.
[40] N. Franke, D. Niewerth, Y. Assaraf, J. Van Meerloo, K. Vojtekova, C. Van Zantwijk, S. Zweegman, E. Chan, C. Kirk, D. Geerke, et al., Impaired bortezomib binding to mutant β5 subunit of the proteasome is the underlying basis for bortezomib resistance in leukemia cells, Leukemia 26 (4) (2012) 757.
[41] S. Lü, J. Wang, The resistance mechanisms of proteasome inhibitor bortezomib, Biomark Res. 1 (1) (2013) 13.
[42] X. Li, Q. Huang, H. Long, P. Zhang, H. Su, J. Liu, A new gold (I) complex- Au (PPh3) PT is a deubiquitinase inhibitor and inhibits tumor growth, EBioMedicine 39 (2019) 159–172.
[43] S. Ciotti, R. Sgarra, A. Sgorbissa, C. Penzo, A. Tomasella, F. Casarsa, F. Benedetti, F. Berti, G. Manfioletti, C. Brancolini, The binding landscape of a partially-selective isopeptidase inhibitor with potent pro-death activity, based on the bis (arylidene) cyclohexanone scaffold, Cell Death Dis. 9 (2) (2018) 184.
[44] V. Kapuria, L.F. Peterson, D. Fang, W.G. Bornmann, M. Talpaz, N.J. Donato, Deubiquitinase inhibition by small-molecule WP1130 triggers aggresome formation and tumor cell apoptosis, Cancer Res. 70 (22) (2010) 9265–9276.
[45] N. Liu, C. Liu, X. Li, S. Liao, W. Song, C. Yang, C. Zhao, H. Huang, L. Guan, P. Zhang, et al., A novel proteasome inhibitor suppresses tumor growth via targeting both 19S proteasome deubiquitinases and 20S proteolytic peptidases, Nat. Sci. Rep. 4 (2014) 5240.
[46] P. D'Arcy, S. Brnjic, M.H. Olofsson, M. Fryknäs, K. Lindsten, M. De Cesare, P. Perego, B. Sadeghi, M. Hassan, R. Larsson, et al., Inhibition of proteasome deubiquitinating activity as a new cancer therapy, Nat. Med. 17 (12) (2011) 1636.
[47] Z. Tian, P. D'Arcy, X. Wang, A. Ray, Y.T. Tai, Y. Hu, R.D. Carrasco, P. Richardson, S. Linder, D. Chauhan, et al., A novel small molecule inhibitor of deubiquitylating enzyme USP14 and UCHL5 induces apoptosis in multiple myeloma and overcomes bortezomib resistance, Blood 123 (5) (2014) 706–716.
[48] X. Wang, M. Mazurkiewicz, E.K. Hillert, M.H. Olofsson, S. Pierrou, P. Hillertz, J. Gullbo, K. Selvaraju, A. Paulus, S. Akhtar, et al., The proteasome deubiquitinase inhibitor VLX1570 shows selectivity for ubiquitin-specific protease-14 and induces apoptosis of multiple myeloma cells, Nat. Sci. Rep. 6 (2016) 26979.
[49] A. Paulus, S. Akhtar, T. Caulfield, K. Samuel, H. Yousaf, Y. Bashir, S. Paulus, D. Tran, R. Hudec, D. Cogen, et al., Coinhibition of the deubiquitinating enzymes, USP14 and UCHL5, with VLX1570 is lethal to ibrutinib- or bortezomib-resistant Waldenstrom macroglobulinemia tumor cells, Blood Canc. J. 6 (11) (2016) e492.
[50] K.N. Kropp, S. Maurer, K. Rothfelder, B.J. Schmied, K.L. Clar, M. Schmidt, B. Strunz, H.G. Kopp, A. Steinle, F. Grünebach, et al., The novel deubiquitinase inhibitor b-AP15 induces direct and NK cell-mediated antitumor effects in human mantle cell lymphoma, Cancer Immunol. Immunother. 67 (6) (2018) 935–947.
[51] R. Didier, A. Mallavialle, R.B. Jouira, M.A. Domdom, M. Tichet, P. Auberger, F. Luciano, M. Ohanna, S. Tartare-Deckert, M. Deckert, Targeting the proteasome-associated deubiquitinating enzyme USP14 impairs melanoma cell survival and overcomes resistance to MAPK-targeting therapies, Mol. Canc. Therapeut. 17 (7) (2018) 1416–1429.
[52] S. Brnjic, M. Mazurkiewicz, M. Fryknäs, C. Sun, X. Zhang, R. Larsson, P. D'Arcy, S. Linder, Induction of tumor cell apoptosis by a proteasome deubiquitinase inhibitor is associated with oxidative stress, Antioxidants Redox Signal. 21 (17) (2014) 2271–2285.
[53] M. Mazurkiewicz, E.K. Hillert, X. Wang, P. Pellegrini, M.H. Olofsson, K. Selvaraju, P. D'Arcy, S. Linder, Acute lymphoblastic leukemia cells are sensitive to disturbances in protein homeostasis induced by proteasome deubiquitinase inhibition, Oncotarget 8 (13) (2017) 21115.
[54] K. Chitta, A. Paulus, S. Akhtar, M.K.K. Blake, T.R. Caulfield, A.J. Novak, S.M. Ansell, P. Advani, S. Ailawadhi, T. Sher, et al., Targeted inhibition of the deubiquitinating enzymes, USP14 and UCHL5, induces proteotoxic stress and apoptosis in Waldenstrom macroglobulinaemia tumour cells, Br. J. Haematol. 169 (3) (2015) 377–390.
[55] D. Sarhan, E. Wennerberg, P. D'Arcy, D. Gurajada, S. Linder, A. Lundqvist, A novel inhibitor of proteasome deubiquitinating activity renders tumor cells sensitive to TRAIL-mediated apoptosis by natural killer cells and T cells, Cancer Immunol. Immunother. 62 (8) (2013) 1359–1368.
[56] X. Zhang, P. Pellegrini, A.A. Saei, E.K. Hillert, M. Mazurkiewicz, M.H. Olofsson, R.A. Zubarev, P. D'Arcy, S. Linder, The deubiquitinase inhibitor b-AP15 induces strong proteotoxic stress and mitochondrial damage, Biochem. Pharmacol. 156 (2018) 291–301.
[57] W. Qinyang, U.J. Lindgren, K. Hultenby, Distribution of galanin in bone and joint tissues, Anat. Embryol. 209 (3) (2005) 227–231.
[58] G. Bjørkøy, T. Lamark, A. Brech, H. Outzen, M. Perander, A. Øvervatn, H. Stenmark, T. Johansen, p62/SQSTM1 forms protein aggregates degraded by autophagy and has a protective effect on huntingtin-induced cell death, J. Cell Biol. 171 (4) (2005) 603–614.
[59] R. Garcia-Mata, Z. Bebök, E.J. Sorscher, E.S. Sztul, Characterization and dynamics of aggresome formation by a cytosolic GFP-chimera, J. Cell Biol. 146 (6) (1999) 1239–1254.
[60] Y. Saeki, Ubiquitin recognition by the proteasome, J. Biochem. 161 (2) (2017) 113–124.
[61] S. Elsasser, D. Chandler-Militello, B. Müller, J. Hanna, D. Finley, Rad23 and Rpn10 serve as alternative ubiquitin receptors for the proteasome, J. Biol. Chem. 279 (26) (2004) 26817–26822.
[62] H. Meyer, C.C. Weihl, The VCP/p97 system at a glance: connecting cellular function to disease pathogenesis, J. Cell Sci. 127 (8) (2014) 3877–3883.
[63] G. Matsumoto, T. Inobe, T. Amano, K. Murai, N. Nukina, N. Mori, N-Acyldopamine induces aggresome formation without proteasome inhibition and enhances protein aggregation via p62/SQSTM1 expression, Nat. Sci. Rep. 8 (1) (2018) 9585.
[64] C. Zhang, J. Gao, M. Li, Y. Deng, C. Jiang, p38δ MAPK regulates aggresome biogenesis by phosphorylating SQSTM1 in response to proteasomal stress, J. Cell Sci. 131 (14) (2018) jcs–216671.
[65] C. Hubbert, A. Guardiola, R. Shao, Y. Kawaguchi, A. Ito, A. Nixon, M. Yoshida, X.F. Wang, T.P. Yao, HDAC6 is a microtubule-associated deacetylase, Nature 417 (6887) (2002) 455.
[66] C. Yu, M. Rahmani, D. Conrad, M. Subler, P. Dent, S. Grant, The proteasome inhibitor bortezomib interacts synergistically with histone deacetylase inhibitors to induce apoptosis in Bcr/Abl+ cells sensitive and resistant to STI571, Blood 102 (10) (2003) 3765–3774.
[67] U. Heider, Metzler Iv, M. Kaiser, M. Rosche, J. Sterz, S. Rötzer, J. Rademacher, C. Jakob, C. Fleissner, U. Kuckelkorn, et al., Synergistic interaction of the histone deacetylase inhibitor SAHA with the proteasome inhibitor bortezomib in mantle cell lymphoma, Eur. J. Haematol. 80 (2) (2008) 133–142.
[68] Q. Zhang, L. Wang, Y. Zhang, X. Jiang, F. Yang, W. Wu, A. Janin, Z. Chen, Z. Shen, S. Chen, et al., The proteasome inhibitor bortezomib interacts synergistically with the histone deacetylase inhibitor suberoylanilide hydroxamic acid to induce T-leukemia/lymphoma cells apoptosis, Leukemia 23 (8) (2009) 1507.
[69] N. Birsa, R. Norkett, N. Higgs, G. Lopez-Domenech, J.T. Kittler, Mitochondrial trafficking in neurons and the role of the Miro family of GTPase proteins, Biochem. Soc. Trans. 41 (6) (2013) 1525–1531.
[70] K.M. Mills, M.G. Brocardo, B.R. Henderson, APC binds the Miro/Milton motor complex to stimulate transport of mitochondria to the plasma membrane, Mol. Biol. Cell 27 (3) (2016) 466–482.
[71] D.C. Altieri, Mitochondria on the move: emerging paradigms of organelle trafficking in tumour plasticity and metastasis, Br. J. Canc. 117 (3) (2017) 301.
[72] A. Melkov, U. Abdu, Regulation of long-distance transport of mitochondria along microtubules, Cell. Mol. Life Sci. 1–14 (2017).
[73] C.J. Decker, R. Parker, P-bodies and stress granules: possible roles in the control of translation and mRNA degradation, Perspect. Biol. (2012) a012286.
[74] H.S. Chahar, S. Chen, N. Manjunath, P-body components LSM1, GW182, DDX3, DDX6 and XRN1 are recruited to WNV replication sites and positively regulate viral replication, Virology 436 (1) (2013) 1–7.
[75] S. de Vries, I.S. Naarmann-de Vries, H. Urlaub, H. Lue, J. Bernhagen, D.H. Ostareck, A. Ostareck-Lederer, Identification of DEAD-box RNA Helicase 6 (DDX6) as a cellular modulator of vascular endothelial growth factor expression under hypoxia, J. Biol. Chem. 288 (8) (2013) 5815.
[76] T.J. Sweet, B. Boyer, W. Hu, K.E. Baker, J. Coller, Microtubule disruption stimulates P-body formation, RNA 13 (4) (2007) 493–502.
[77] A. Aizer, Y. Brody, L.W. Ler, N. Sonenberg, R.H. Singer, Y. Shav-Tal, The dynamics of mammalian P-body transport, assembly, and disassembly in vivo, Mol. Biol. Cell 19 (10) (2008) 4154–4166.
[78] D. Rajgor, C.M. Shanahan, RNA granules and cytoskeletal links, Biochem. Soc. Trans. 42 (4) (2014) 1206–1210.
[79] F. Bärenz, D. Inoue, H. Yokoyama, J. Tegha-Dunghu, S. Freiss, S. Draeger, D. Mayilo, I. Cado, S. Merker, M. Klinger, et al., The centriolar satellite protein SSX2IP promotes centrosome maturation, J. Cell Biol. 202 (1) (2013) 81–95.
[80] M. Itoh, C.H. Kim, G. Palardy, T. Oda, Y.J. Jiang, D. Maust, S.Y. Yeo, K. Lorick, G.J. Wright, L. Ariza-McNaughton, et al., Mind bomb is a ubiquitin ligase that is essential for efficient activation of Notch signaling by Delta, Dev. Cell 4 (1) (2003) 67–82.
[81] J.B. Woodruff, O. Wueseke, A.A. Hyman, Pericentriolar material structure and dynamics, Phil. Trans. Roy. Soc. B 369 (1650) (2014) 20130459.
[82] B.H. Villumsen, J.R. Danielsen, L. Povlsen, K.B. Sylvestersen, A. Merdes, P. Beli, Y.G. Yang, C. Choudhary, M.L. Nielsen, N. Mailand, et al., A new cellular stress response that triggers centriolar satellite reorganization and ciliogenesis, EMBO J. 32 (23) (2013) 3029–3040.
[83] Z. Tang, M.G. Lin, T.R. Stowe, S. Chen, M. Zhu, T. Stearns, B. Franco, Q. Zhong, Autophagy promotes primary ciliogenesis by removing OFD1 from centriolar satellites, Nature 502 (7470) (2013) 254.
[84] K. Kim, K. Lee, K. Rhee, CEP90 is required for the assembly and centrosomal accumulation of centriolar satellites, which is essential for primary cilia formation, PLoS One 7 (10) (2012) e48196.
[85] H. Bouguenina, D. Salaun, A. Mangon, L. Muller, E. Baudelet, L. Camoin, T. Tachibana, S. Cianferani, S. Audebert, P. Verdier-Pinard, et al., EB1- binding–myomegalin protein complex promotes centrosomal microtubules functions, Proc. Natl. Acad. Sci. 114 (50) (2017) E10687–E10689.
[86] M.B. Yaffe, G.W. Farr, D. Miklos, A.L. Horwich, M.L. Sternlicht, H. Sternlicht, TCP1 complex is a molecular chaperone in tubulin biogenesis, Nature 358 (6383) (1992) 245.
[87] A. Leitner, L.A. Joachimiak, A. Bracher, L. Mönkemeyer, T. Walzthoeni, B. Chen, S. Pechmann, S. Holmes, Y. Cong, B. Ma, et al., The molecular architecture of the eukaryotic chaperonin TRiC/CCT, Structure 20 (5) (2012) 814–825.
[88] S.H. Roh, M. Kasembeli, D. Bakthavatsalam, W. Chiu, D.J. Tweardy, Contribution

of the type II chaperonin, TRiC/CCT, to oncogenesis, Int. J. Mol. Sci. 16 (11) (2015) 26706–26720.
[89] J.W. Francis, L.E. Newman, L.A. Cunningham, R.A. Kahn, A trimer consisting of the Tubulin-specific Chaperone D (TBCD), regulatory GTPase ARL2, and b-tubulin is required for maintaining the microtubule network, J. Biol. Chem. 292 (10) (2017) 4336.
[90] L.M. Fujimoto, R. Roth, J.E. Heuser, S.L. Schmid, Actin assembly plays a variable, but not obligatory role in receptor-mediated endocytosis, Traffic 1 (2) (2000) 161–171.
[91] H. Hehnly, M. Stamnes, Regulating cytoskeleton-based vesicle motility, FEBS Lett. 581 (11) (2007) 2112–2118.
[92] E.A. Obeng, L.M. Carlson, D.M. Gutman, W.J. Harrington, K.P. Lee, L.H. Boise, Proteasome inhibitors induce a terminal unfolded protein response in multiple myeloma cells, Blood 107 (12) (2006) 4907–4916.
[93] E. Aleo, C.J. Henderson, A. Fontanini, B. Solazzo, C. Brancolini, Identification of new compounds that trigger apoptosome-independent caspase activation and apoptosis, Cancer Res. 66 (18) (2006) 9235–9244.
[94] A. Tomasella, R. Picco, S. Ciotti, A. Sgorbissa, E. Bianchi, R. Manfredini, F. Benedetti, V. Trimarco, F. Frezzato, L. Trentin, et al., The isopeptidase inhibitor 2cPE triggers proteotoxic stress and ATM activation in chronic lymphocytic leukemia cells, Oncotarget 7 (29) (2016) 45429.
[95] L. Santo, T. Hideshima, A.L. Kung, J.C. Tseng, D. Tamang, M. Yang, M. Jarpe, J.H. van Duzer, R. Mazitschek, W.C. Ogier, et al., Preclinical activity, pharmacodynamic and pharmacokinetic properties of a selective HDAC6 inhibitor, ACY-1215, in combination with bortezomib in multiple myeloma, Blood 119 (11) (2012) 2579–2589.
[96] V. Seiberlich, O. Goldbaum, V. Zhukareva, C. Richter-Landsberg, The small molecule inhibitor PR-619 of deubiquitinating enzymes affects the micro- tubule network and causes protein aggregate formation in neural cells: implications for neurodegenerative diseases, Biochim. Biophys. Acta Mol. Cell Res. 1823 (11) (2012) 2057–2068.
[97] N. Zaarur, X. Xu, P. Lestienne, A.B. Meriin, M. McComb, C.E. Costello, G.P. Newnam, R. Ganti, N.V. Romanova, M. Shanmugasundaram, et al., RuvbL1 and RuvbL2 enhance aggresome formation and disaggregate amyloid fibrils, EMBO J. (2015) e201591245.
[98] H. Herrmann, U. Aebi, Intermediate filaments: molecular structure, assembly mechanism, and integration into functionally distinct intracellular scaffolds, Annu. Rev. Biochem. 73 (1) (2004) 749–8.
[99] V. Prahlad, M. Yoon, R.D. Moir, R.D. Vale, R.D. Goldman, Rapid movements of vimentin on microtubule tracks: kinesin-dependent assembly of intermediate filament networks, J. Cell Biol. 143 (1) (1998) 159–170.
[100] B.T. Helfand, A. Mikami, R.B. Vallee, R.D. Goldman, A requirement for cytoplasmic dynein and dynactin in intermediate filament network assembly and organization, J. Cell Biol. 157 (5) (2002) 795–806.
[101] M. Guo, A.J. Ehrlicher, S. Mahammad, H. Fabich, M.H. Jensen, J.R. Moore, J.J. Fredberg, R.D. Goldman, D.A. Weitz, The role of vimentin intermediate filaments in cortical and cytoplasmic mechanics, Biophys. J. 105 (7) (2013) 1562–1568.
[102] F.K. Gyoeva, V.I. Gelfand, Coalignment of vimentin intermediate filaments with microtubules depends on kinesin, Nature 353 (6343) (1991) 445.